minerals

MDPI

Article

Retardation of Chlorine-36 by Cementitious Materials Relevant to the Disposal of Radioactive Wastes

Matthew Isaacs [1,2,3], Steve Lange [1,4], Antoni E. Milodowski [5], Dirk Bosbach [1], David Read [2] and Guido Deissmann [1,*]

[1] Department of Nuclear Waste Management (IFN-2), Institute of Fusion Energy and Nuclear Waste Management (IFN), Forschungszentrum Jülich GmbH, 54248 Jülich, Germany; matthew.isaacs@mottmac.com (M.I.); steve.lange@bge.de (S.L.); d.bosbach@fz-juelich.de (D.B.)
[2] School of Chemistry and Chemical Engineering, University of Surrey, Guildford GU2 7XH, UK; d.read@surrey.ac.uk
[3] Mott MacDonald Ltd., 10 Temple Back, Bristol BS1 6FL, UK
[4] BGE Bundesgesellschaft für Endlagerung mbH, Schachtanlage Asse II, 38319 Remlingen, Germany
[5] British Geological Survey (BGS), Keyworth, Nottingham NG12 5GG, UK; aem.amethystgeo@virginmedia.com
* Correspondence: g.deissmann@fz-juelich.de; Tel.: +49-2461-61-2556

Abstract: The activation product chlorine-36 (^{36}Cl) is an important radionuclide within the context of the disposal of nuclear wastes, due to its long half-life and environmental mobility. Its behaviour in a range of potential cementitious encapsulants and backfill materials was studied by evaluating its uptake by pure cement hydration phases and hardened cement pastes (HCP). Limited uptake of chloride was observed on calcium silicate hydrates (C-S-H) by electrostatic sorption and by calcium monosulphoferroaluminate hydrate (AFm) phases, due to anion exchange/solid solution formation. Diffusion of ^{36}Cl through cured monolithic HCP samples, representative of cementitious materials considered for use in deep geological repositories across Europe, revealed a markedly diverse migration behaviour. Two of the matrices, a ground granulated blast furnace slag/ordinary Portland cement blend (GGBS–OPC) and an ordinary Portland cement (CEM I) effectively retarded ^{36}Cl migration, retaining the radionuclide in narrow, reactive zones. The migration behaviour of ^{36}Cl within the cementitious matrices is not strictly correlated to the measured sorption distribution ratios (R_d-values), suggesting that physical factors related to the microstructure can also have a distinct effect on diffusion behaviour. The findings have implications when selecting cementitious grouts and/or backfill materials for ^{36}Cl-bearing radioactive wastes.

Keywords: cementitious materials; radioactive waste; chlorine-36; sorption

Citation: Isaacs, M.; Lange, S.; Milodowski, A.E.; Bosbach, D.; Read, D.; Deissmann, G. Retardation of Chlorine-36 by Cementitious Materials Relevant to the Disposal of Radioactive Wastes. *Minerals* **2024**, *14*, 1017. https://doi.org/10.3390/min14101017

Academic Editor: James Begg

Received: 23 August 2024
Revised: 1 October 2024
Accepted: 3 October 2024
Published: 9 October 2024

1. Introduction

Cementitious materials are in widespread use in the management of radioactive wastes. They are employed, for example, for conditioning and solidification of low- and intermediate-level radioactive wastes, as material for specific waste containers, and/or as construction, backfill, and sealing materials in near-surface and deep geological disposal facilities for radioactive wastes (e.g., [1–4]). Depending on the scope of the application, various cement formulations are in use or under consideration for future usage, such as Ordinary Portland cements (OPC), cements containing ground/granulated blast furnace slags (GGBS) and/or fly ash (FA), as well as supplementary cementitious materials such as silica fume (SF). In the last two decades, the use of low alkalinity cementitious materials ("low-pH cements") has been increasingly explored, aiming at minimising potential deleterious effects of highly alkaline cement pore waters ("alkaline plume") on clay-based materials (e.g., bentonite or clay host rocks) in the repository near-field (e.g., [5–8]). Cementitious materials are heterogeneous mixtures of various cement hydration phases, in

particular, predominantly nanocrystalline calcium–silicate–hydrates (C-S-H), some hydrated sulphate containing calcium aluminate/ferrate compounds (AFm/AFt), portlandite ($Ca(OH)_2$), and some minor phases such as hydrotalcite (cf. [9,10]). The amounts and the composition of the hydration phases (e.g., the Ca/Si ratio of C-S-H or their Al and alkali content) in specific cementitious materials and their microstructure (e.g., porosity, pore structure, and diffusivity) are a function of the cement types employed and the environmental conditions during mixing and curing [10].

Various processes can contribute to the retention of radionuclides in cementitious materials and effect radionuclide migration in the repository environment: (i) precipitation of sparingly soluble solids, (ii) (ad)sorption processes on the surfaces of hydration phases, (iii) ion exchange (e.g., anion exchange with interlayer anions in AFm phases), and/or (iv) incorporation into pre-existing or newly formed solids (e.g., by entrapment during coprecipitation or recrystallisation and/or by solid solution formation). The extent of radionuclide uptake depends on the nature, valence state and speciation of the radionuclide, the environmental conditions and pore water composition (e.g., pH, redox conditions, temperature, ionic strength, carbonate content/pCO_2, etc.), the type of cementitious materials and their degradation state, and the use of cement additives such as superplasticisers (e.g., [11]). The uptake of radionuclides by cementitious materials has been addressed in numerous studies during the last decades, often on a phenomenological basis (e.g., reviews in [1,12–14]) resulting in the development of various sorption databases (e.g., [11,14–18]) used in safety assessments. The potential of the high-pH cementitious environment to reduce the solubility and mobility of various (cationic) radionuclides is well established. However, the retention of anionic species has not been studied to the same extent. Thus, in safety assessments, it is often assumed that anionic species of safety-relevant radionuclides such as ^{129}I, ^{36}Cl, or ^{79}Se will be much more mobile in the repository near and far field (e.g., [19,20]).

^{36}Cl is a long-lived beta-emitting radionuclide with a half-life of 3.01 (± 0.02)·× 10^5 years [21] that is produced in nuclear reactors by neutron capture (neutron activation) from the stable natural chlorine isotope ^{35}Cl. Owing to the high cross section of this nuclear reaction, even trace amounts of ^{35}Cl in structural reactor materials or nuclear fuels can lead to significant amounts of ^{36}Cl if the neutron flux is sufficient. The majority of ^{36}Cl inventory is found in spent nuclear fuels rather than in vitrified high-level waste from reprocessing due to volatilisation. Conversely, intermediate-level reprocessing wastes such as hulls and end pieces retain their original ^{36}Cl inventory. In low-level wastes, ^{36}Cl is mainly found in stainless reactor steels and other metals, i.e., ^{36}Cl can be distributed over many radioactive waste streams from nuclear reactors (cf. [22]).

In aqueous environments, chlorine exists generally in the form of chloride (Cl^-). The uptake process of Cl^- in hardened cement paste (HCP) is still poorly understood [17,22,23]. The binding of ^{36}Cl to HCP is generally rather weak and was found to decrease with increasing concentration of stable Cl^- in solution [11,17]; thus, ^{36}Cl is often assumed to be poorly or non-retarded in safety assessments. Several mechanisms for Cl^- retention by HCP have been proposed (cf. [11,13]). Chemisorption was considered to control Cl^- retention by C-S-H phases in particular at Ca/Si ratios > 1.2 when the C-S-H surface was positively charged (e.g., [24–26]). This is the case in young cementitious systems, in particular, in OPC-rich cement formulations, whereas, in low-pH cementitious materials and in degraded systems (i.e., after depletion of the portlandite buffer), C-S-H with lower Ca/Si ratios prevails. Moreover, Cl^- can react with unhydrated aluminate phases to form AFm-type compounds ($Ca_4Al_2(OH)_{12}(X^{2-})\cdot 6H_2O$) such as Friedel's salt ($Ca_2Al(OH)_6(Cl,OH)\cdot 2H_2O$), in particular, at higher Cl^- concentrations in the porewater (cf. [11,13,27–29]). In carbonate-containing cements, the binding by AFm phases is thought to be predominantly due to the formation of a solid–solution between calcium mono-carboaluminate ($Ca_4Al_2(OH)_{12}CO_3\ 5H_2O$) and Friedel's salt [17,22]. Cl^- may also substitute for OH^- in the interlayer of hydrotalcite ($Mg_6Al_2CO_3(OH)_{16}\cdot 4H_2O$) [11,30], though its uptake capacity for Cl^- is deemed to be limited due to the small amounts usually present in HCP

[17]. Van Es et al. [29] observed binding of Cl^- to partially hydrated glassy, sulphate-bearing calcium silicate clinker particles in the matrix as an important retardation mechanism in a specific cementitious material (Nirex Reference Vault Backfill, NRVB), which has been considered as a candidate backfill material for a geological disposal facility in the UK.

The aim of the present work is to provide further insights into the migration behaviour of anionic halogen species in cementitious materials by investigating (i) the retention of chloride ions by individual cement hydration phases and different HCPs and (ii) diffusion of ^{36}Cl through cured monolithic HCP samples, representative for cementitious materials considered for use in geological disposal facilities across Europe.

2. Materials and Methods

2.1. Cementitious Materials

The materials employed in this study fall into two categories: synthesised cement hydration phases and crushed HCP were used in batch sorption tests; monolithic HCP samples were employed for through-diffusion studies. The synthesised cement hydration phases comprised C-S-H with a Ca/Si ratio of 0.9 (termed C-S-H0.9) and two AFm phases, namely monosulphate (AFm-SO_4) and monocarbonate (AFm-CO_3). C-S-H with a low Ca/Si ratio was employed to mimic conditions in slightly degraded cement and C-S-H formed in blended cements, respectively. Established synthesis routes from the literature were used for the synthesis of C-S-H [31] and AFm phases [32,33]; details of the procedures are described elsewhere [34,35]. Synthesis of the hydration phases, sample preparation, and storage were performed in an inert gas glove box (Ar atmosphere; < 10 ppm CO_2) to avoid carbonation. The purity of the synthesised phases was assessed by powder X-ray diffraction spectroscopy (XRD), using either a D4 Endeavor (Bruker AXS GmbH, Karlsruhe, Germany) with a θ-2θ geometry or a D8 Advance (Bruker AXS GmbH) with a θ-θ geometry, employing CuKα radiation; the results revealed synthesis of pure phases in all cases. In addition, microstructural/microchemical investigations were performed by scanning electron microscopy SEM (FEI Quanta 200F, FEI, Eindhoven, The Netherlands) equipped with a field emission cathode and energy-dispersive X-ray spectroscopy (EDS) using an Apollo X Silicon Drift Detector (SDD) from EDAX (Weiterstadt, Germany). SEM/EDS analyses were performed in low-vacuum mode (60 Pa) to avoid coating of the samples with gold or carbon. A detailed characterisation of the synthesised hydration phases is provided elsewhere [34,35], summarised in the Supplementary Materials (Figures S1 to S3). The specific surface areas of the synthesised phases were determined by multipoint N_2-BET measurements, employing a Quantachrome Autosorb 1 (Quantachrome GmbH, Odelzhausen, Germany); the Quantachrome AS1Win (v. 2.11) software was used for data treatment, revealing specific surface areas of 126 $m^2\,g^{-1}$ for C-S-H0.9 and 1.1 $m^2\,g^{-1}$ for AFm-SO_4 [36]; the specific surface area of AFm-CO_3 was not determined.

In the through-diffusion study, five cement formulations were used, including an OPC (CEM I 42.5N), a pulverised fuel ash/OPC blend (PFA–OPC), a ground granulated blast furnace slag/OPC blend (GGBS–OPC), the candidate cementitious backfill material Nirex Reference Vault Backfill (NRVB, [37]), and a low-pH reference cement blend used for benchmarking purposes in the European Cebama project [4], provided by VTT, Finland [38,39]. The basis of the latter was a ternary mix design containing OPC, GGBS, SF, and quartz filler that had been used successfully in full-scale demonstrations for deposition tunnel end plugs in crystalline rocks in Finland [40,41]. Waste management organisations in many countries (e.g., Switzerland, France, Belgium, and Finland) intend to use CEM-I-based cement formulations (often as blended cements with fly ash, blast furnace slag, and other supplementary cementitious materials) in their repository concepts.

The formulations used for the preparation of each of the HCP samples are detailed in Table 1; additional information on the chemical composition of the different constituents is included in Table S1 in the Supplementary Materials. The powders were mixed in

a bench-top conical mixer in a polypropylene hexagonal barrel (Pascall Lab-mixer II, Pascall Engineering, Crawley, UK) until homogeneous.

Table 1. Formulations of HCP samples (mass fractions) used in sorption and through-diffusion experiments.

Blend	OPC	PFA	GGBS	Hydrated Lime	Lime Flour	Silica Fume	Quartz Filler	w/c[1]
CEM I	1							0.45
PFA–OPC	1	3						0.45
GGBS–OPC	1		9					0.45
NRVB	1			0.38	1.1			0.55
Cebama	1		0.62			0.87	1.1	0.45

[1] w/c: water/cement ratio (by mass).

For preparation of the HCP monoliths for the through-diffusion experiments, each of the cement blends was mixed with the respective pre-equilibrated solution at a w/c ratio of 0.45 or 0.55 (NRVB). The fresh pastes were poured into cylindrical polypropylene containers (volume 50 mL) and left to set for 24 h. After removing the cylinders (diameter: 40 mm; length of 40 to 45 mm) from the moulds, the samples were cured in sealed containers for 28 days. After the curing period, a well (diameter: 10 mm; depth: 30 mm) was drilled centrally along the longitudinal axis of the cylinders; the top and bottom surfaces of the cylinders were sealed with wax (Figure 1).

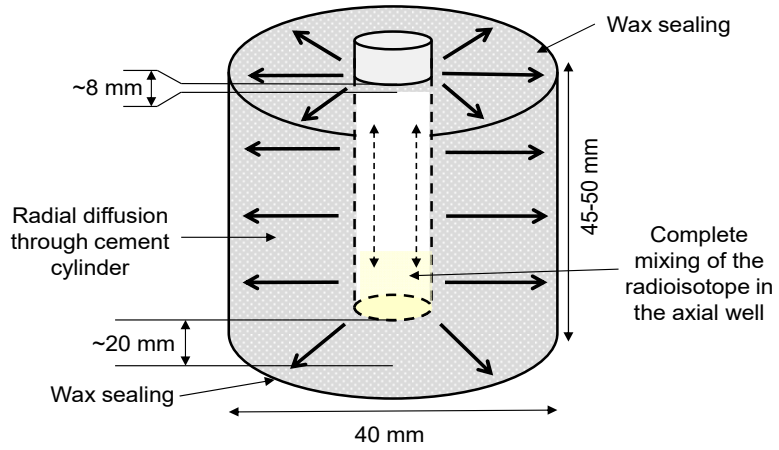

Figure 1. Schematic of the radial diffusion experiments using HCP cylinders.

Pre-equilibrated waters for use in sorption and diffusion experiments were prepared by mixing crushed HCP (grain size < 2 mm) with deionised water at an S/L ratio of 0.05 kg L^{-1} under N_2 atmosphere. The suspensions were stored for 28 days and agitated daily to prevent sedimentation; subsequently, the solids were removed by filtration and the solutions analysed by ion chromatography (cf. Table S2 in the Supplementary Materials). These waters are equilibrated with HCP partially degraded due to leaching. Thus, the pH of the CEM I equilibrated water is relatively low (pH 12.8) compared to the typical pore water in young CEM I HCP with a pH of ~13.3.

2.2. Batch Sorption Experiments

Sorption of stable Cl^- to the synthesised hydration phases and crushed HCP were determined in batch experiments under anoxic conditions, achieved by performing all experiments in inert gas glove boxes (either under Ar or N_2). Sorption and diffusion experiments were conducted at room temperature (20 to 23 °C), which is of the same order as in

deep geological repositories at depths of about 500 m after the thermal phase, when ambient conditions have been restored (assuming a typical geothermal gradient of 30 K km^{-1}).

The sorption experiments were performed in 20 mL LDPE bottles. For the batch experiments with the synthesised hydration phases, solutions pre-equilibrated with the respective solids were used. Therefore, defined amounts of the solids (0.005 kg L^{-1}) were equilibrated with deionised water (18.2 MΩ) for 14 days under anoxic conditions; afterwards, solid and liquid phases were separated by filtration. The pH of the equilibrated solutions is given in Table S3 in the Supplementary Materials.

In the sorption experiments, fresh model phases were added to the solutions (S/L = 0.01 kg L^{-1}) and stored for 14 days. Then, inactive Cl^- was added in the form of KCl at a concentration of 10^{-3} mol L^{-1}; the bottles were shaken by hand regularly. The timeframe of the experiments to determine equilibrium R_d values (i.e., 40 days) was selected in line with the outcome of similar studies [42]. Prior to the analysis of the solution, liquid and solids were separated by filtration using USY-1 ultrafilters (10,000 Da, Advantec MFS, Dublin, California, USA). Chloride concentrations were determined by ion chromatography using a Dionex ICS-5000 system (ThermoFisher Scientific, Waltham, Massachusetts, USA). Prior to the uptake experiments, Cl^- sorption to reaction vessels and filters had been tested and found to be negligible. The sorption experiments with crushed HCP (< 2 mm) were performed in a similar manner (e.g., duration 40 days) to the experiments with the hydration phases at an S/L ratio of 0.02 kg L^{-1} using solutions that had been pre-equilibrated with the crushed HCP material.

The uptake of Cl^- by the solids was evaluated and quantified in terms of the distribution ratio (R_d) between the amount of Cl^- sorbed by the solids (Cl_{sorbed}; mol kg^{-1}) and the amount remaining in solution ($A_{solution}$; mol L^{-1}) as:

$$R_d = \frac{Cl_{sorbed}}{Cl_{solution}} \quad (1)$$

calculated as:

$$R_d = \frac{C_i - C_t}{C_t} \frac{V}{m} \quad (2)$$

Here, C_i is the initial Cl^- concentration in solution (mol L^{-1}), C_t the concentration at time t (mol L^{-1}), V the volume of the liquid phase (L), and m the mass of the solid phase (kg) used in the experiment. In the experiments with HCP, the background Cl^- concentration of the solutions was taken into account in the calculation of the R_d values. All sorption experiments were carried out in triplicate. Uncertainties in the R_d values were estimated from propagated uncertainties associated with the experimental procedures (e.g., weighing, pipetting, etc.) and those resulting from the solution analysis, using Gaussian error propagation.

2.3. Through-Diffusion Experiments

The radial diffusion of ^{36}Cl through the cured HCP cylinders was assessed using an experimental protocol described previously [29,43,44]. Pre-equilibrated cement waters (volume 1 mL) containing 11.9 kBq ^{36}Cl (as chloride, corresponding to $2.71 \cdot 10^{-4}$ mol L^{-1} Cl^-) were spiked into the central wells of the cylinders (Figure 1), filling them approximately halfway. After sealing of the wells, the cylinders were submerged in 200 mL of the same pre-equilibrated water and kept under N_2 atmosphere in a glove box throughout the experiments and during sampling. All experiments were carried out in duplicate.

The diffusive migration of $^{36}Cl^-$ through the HCP cylinders was monitored by measuring the activity concentration in the solution surrounding the cylinders. Sampling by taking 1 cm^3 aliquots was initially performed on a daily basis and, later, weekly. The solutions were filtered prior to analysis through qualitative cellulose filters (Thermo Fisher Scientific; 11 μm particle retention). The activity concentration in the samples was determined by liquid scintillation counting (LSC) using a 2100TR Liquid Scintillation Analyzer

(Packard Instrument Company, Meriden, Connecticut, USA) in the energy range between 20 and 200 keV after the addition of a liquid scintillation cocktail (Goldstar, Meridian, UK). Similar through-diffusion experiments were carried out for each HCP formulation using a nominally conservative tracer, namely tritiated water (HTO). Here, a total activity of ca. 5000 Bq was added to the central well of each of the HCP cylinders. As in the case of ^{36}Cl, HTO diffusion through the HCP was assessed in duplicate; breakthrough was determined by LSC measurements. Dimensionless "relative" retardation factors *(Rf,* i.e., relative with respect to HTO) with respect to the diffusive transport of ^{36}Cl were calculated by:

$$Rf = \frac{C_{t,\,HTO}/C_{0,\,HTO}}{C_{t,\,Cl\text{-}36}/C_{0,\,Cl\text{-}36}} \quad (3)$$

where C_0 refers to the initial activity concentrations (Bq L^{-1}) of HTO and ^{36}Cl, respectively, in the well and C_t to the activity concentration in the surrounding solution at time t.

2.4. Autoradiography

After terminating the through-diffusion experiments, the cylinders were removed from the solution and cut longitudinally with a diamond masonry saw to determine the migration profiles of ^{36}Cl by digital laser-photostimulated luminescence (LPSL) autoradiography, following the methodology described in detail in Isaacs et al. [44]. LPSL autoradiography images were obtained using storage phosphor imaging plates (IP) (Fuji BAS-MP2025P) that comprise a microcrystalline Eu-doped barium fluorobromide ($BaFBr:Eu^{2+}$) photo-stimulable phosphor layer and which cumulatively detect alpha-, beta-, and gamma-radiation as well as background cosmic radiation (for details, see [44]). The flat surfaces of the cut cylinders were directly placed onto the IPs for 4 h in a light-tight box. Prior to this, the central wells in the HCP blocks were filled with dental impression wax to shield the IPs from any interference caused by radiation "shine" from radionuclides present on the 3D internal surface of the well wall. Following exposure, the IP were removed under darkroom conditions and scanned at 50 μm pixel resolution with an Amersham Biosciences (GE Healthcare Ltd., Little Chalfont, Buckinghamshire, UK) STORM™ 860 digital fluorescence laser scanner, using red laser light (635 nm) and a 650 nm low-pass wavelength filter, to record the latent image. Data processing of the LPSL autoradiography images was performed using the ImageQuant TL v.2005 software package (GE Healthcare Ltd.) and the FiJi (ImageJ, (v. 1.48k, December 2013)) public-domain open-source software package [45], coupled with the "Linearise GelData" software "plug-in" (Version 2012/11/06) [46] to produce quantitative linear colour-contoured intensity images (cf. [44]).

3. Results

3.1. Uptake of Cl^- by Cement Hydration Phases and HCP

The uptake of chloride by single cement hydration phases (i.e., C-S-H0.9, AFm-SO_4, and AFm-CO_3) was investigated in batch sorption experiments in equilibrium solutions with pH ranging between 11.3 and 12.0 (Table S2 in the Supplementary Materials). The distribution ratios R_d for the sorption of Cl^- are summarised in Table 2. From the three phases studied, AFm-SO_4 showed the strongest sorption (R_d = 27 ± 0.6 L kg^{-1}), while the uptake on AFm-CO_3 and C-S-H0.9 was lower (R_d = 17 ± 0.2 L kg^{-1}). The differing R_d values for the two AFm phases indicate an impact of the interlayer anion on anion exchange capacity and selectivity, respectively.

Table 2. Distribution ratios R_d for the uptake of Cl^- by cement hydration phases in equilibrium solutions.

Phase	R_d (L kg^{-1})
C-S-H 0.9	17 ± 0.2
AFm-SO_4	27 ± 0.6
AFm-CO_3	17 ± 0.2

The R_d values for Cl^- uptake by the various HCP employed in the through-diffusion experiments, determined on crushed materials, are provided in Table 3. From the batch sorption data, a distinctly stronger uptake of Cl^- by the PFA–OPC based HPC is indicated (R_d = 26 ± 1.3 L kg^{-1}), while the ternary Cebama blend showed the lowest binding capacity for Cl^- (R_d = 6.5 ± 0.1 L kg^{-1}). The similar R_d values for HCP CEM I and the 9:1 GGBS–OPC blend suggest a similar sorption capacity for Cl^- of OPC and GGBS.

Table 3. Distribution ratios R_d for the uptake of Cl^- by HCP.

Binder	R_d (L kg^{-1})
CEM I	11 ± 1.0
PFA–OPC	26 ± 1.3
GGBS–OPC	9.8 ± 0.2
NRVB	7.5 ± 0.5
Cebama	6.5 ± 0.1

3.2. Diffusion of ^{36}Cl through HCP

3.2.1. Through-Diffusion Experiments

For the assessment of physical factors affecting the diffusive transport of solutes in porous media and to compare the transport properties of the different HCP, through-diffusion experiments with HTO, assumed as an "ideal" conservative tracer, were performed for 270 days. As expected, the initial tritium breakthrough occurred rapidly as ^3H was already detected in the samples taken from the solution surrounding the HCP blocks after 24 h (Figure 2). The PFA–OPC and the NRVB blends show the fastest tritium migration, with the ^3H concentration approaching the input level after 14 days (i.e., $C/C_0 \rightarrow 1$). The Cebama reference blend revealed a slightly slower transport rate, reaching a C/C_0 value of 0.8 after 28 days; in the experiments with CEM I and GGBS–OPC, the ^3H concentrations continued to increase until the experiments◎conclusion at 270 days. Assuming that radionuclide migration was not affected by chemical interactions within the HCP, the rate of transport would be expected to decrease in the order PFA–OPC ≈ NRVB > Cebama >> CEM I ≈ GGBS–OPC.

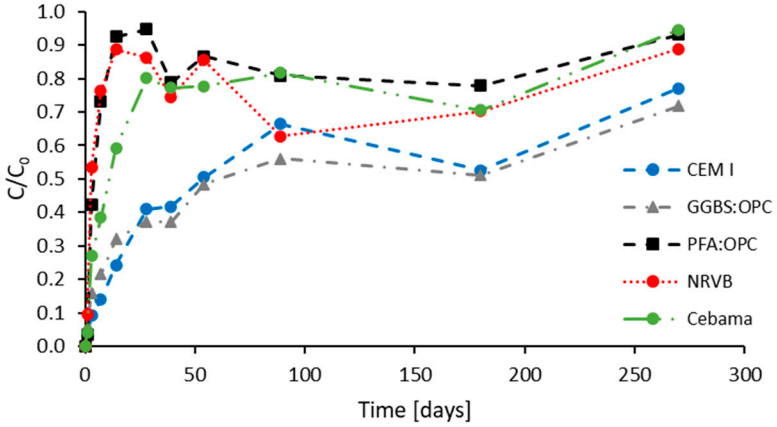

Figure 2. Breakthrough curves for tritiated water (HTO) in through-diffusion experiments using different HCP (error bars are in the order of the size of symbols).

The results of the ^{36}Cl through-diffusion experiments are shown in Figure 3, providing a consistent picture to the findings for the diffusion of HTO. The PFA–OPC and NRVB allowed the fastest migration through the HCP, initially at a very similar rate, albeit C/C_0 values start to diverge around 40 days before reaching C/C_0 values of 0.9 and 0.55, respectively. The Cebama reference blend HCP showed a slower breakthrough, reaching a C/C_0 value of 0.3 after 270 days. The CEM I and GGBS–OPC showed no ^{36}Cl breakthrough over the timescale of the experiment. The ^{36}Cl breakthrough findings are similar to the HTO results, with the rate of chloride transport decreasing in the order PFA–OPC > NRVB > Cebama >> CEM I ≈ GGBS–OPC, implying that HCP permeability is a major factor controlling chlorine transport in HCP. Despite this, the higher variance in the C/C_0 values obtained at the end point of the ^{36}Cl experiments, especially in the HCPs that had similar initial rates of HTO transport (PFA–OPC and NRVB), indicates that there are significant chemical retention processes in the system, which depend strongly on the cement formulation, as indicated in particular by the differences in ^{36}Cl transport through the PFA–OPC, NRVB, and Cebama HPC blocks. The retardation of ^{36}Cl transport compared to the HTO tracer expressed by the retardation factor *Rf* varies from close to 1 (PFA–OPC), i.e., no retardation, up to 62 (CEM I) at the end of the experiments (Table 4).

Table 4. Retardation factors *Rf* for the diffusive transport of $^{36}Cl^-$ through HCP (after 270 days) compared to HTO.

Binder	*Rf* (-)
CEM I	61.5
PFA–OPC	1.0
GGBS–OPC	38.1
NRVB	1.6
Cebama	3.4

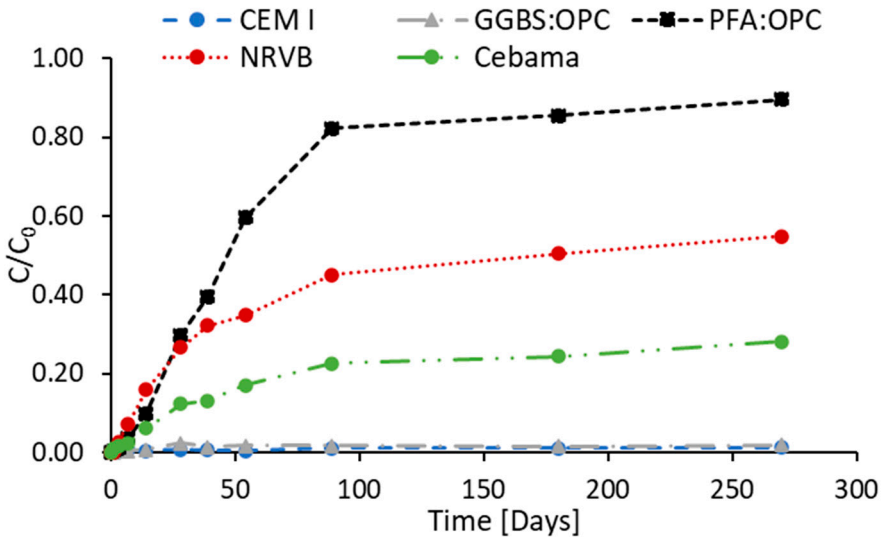

Figure 3. Breakthrough curves for ^{36}Cl in through-diffusion experiments using different HCP (error bars are in the order of the size of symbols).

3.2.2. Autoradiography of HCP Blocks

At the end of the through-diffusion experiments the HPC blocks were cut longitudinally, allowing the migration profile of ^{36}Cl to be imaged and examined from the central well to the outer edge of each block using digital LSPL autoradiography. The autoradiograph images for CEM I (Figure 4a) and GGBS–OPC (Figure 4b) blocks indicate that these HCPs display the strongest retention for ^{36}Cl and that ^{36}Cl migration through the cement matrix has been very limited during the experiment. This is consistent with the results from fluid chemistry (cf. Figure 3). The ^{36}Cl appears to have been largely retained on the well walls and within the immediately adjacent matrix of the HCP. The distribution of ^{36}Cl activity was similar in both CEM I and GGBS–OPC blocks, with peak activity at a depth into the cement of between 0.5 and 1.5 mm in the CEM I block (feature labelled "a" in Figure 4a) and about 1 mm in the GGBS–OPC block (feature labelled "a" in Figure 4b). The ^{36}Cl activity decreases sharply thereafter, approaching background radioactivity levels at between 11 and 12 mm from the well wall in the CEM I block and at about 9 mm in GGBS–OPC block. The autoradiograph produced from the CEM I block also revealed a weakly radioactive linear feature, inclined at about 30° from the vertical and extending from the base of the well towards the edge of the block (feature labelled "b" in Figure 4a(ii)). This appears to correspond to a hairline fracture within the HCP block and suggests that a very minor amount of ^{36}Cl diffusion has occurred along this microfracture flaw feature in this cement block.

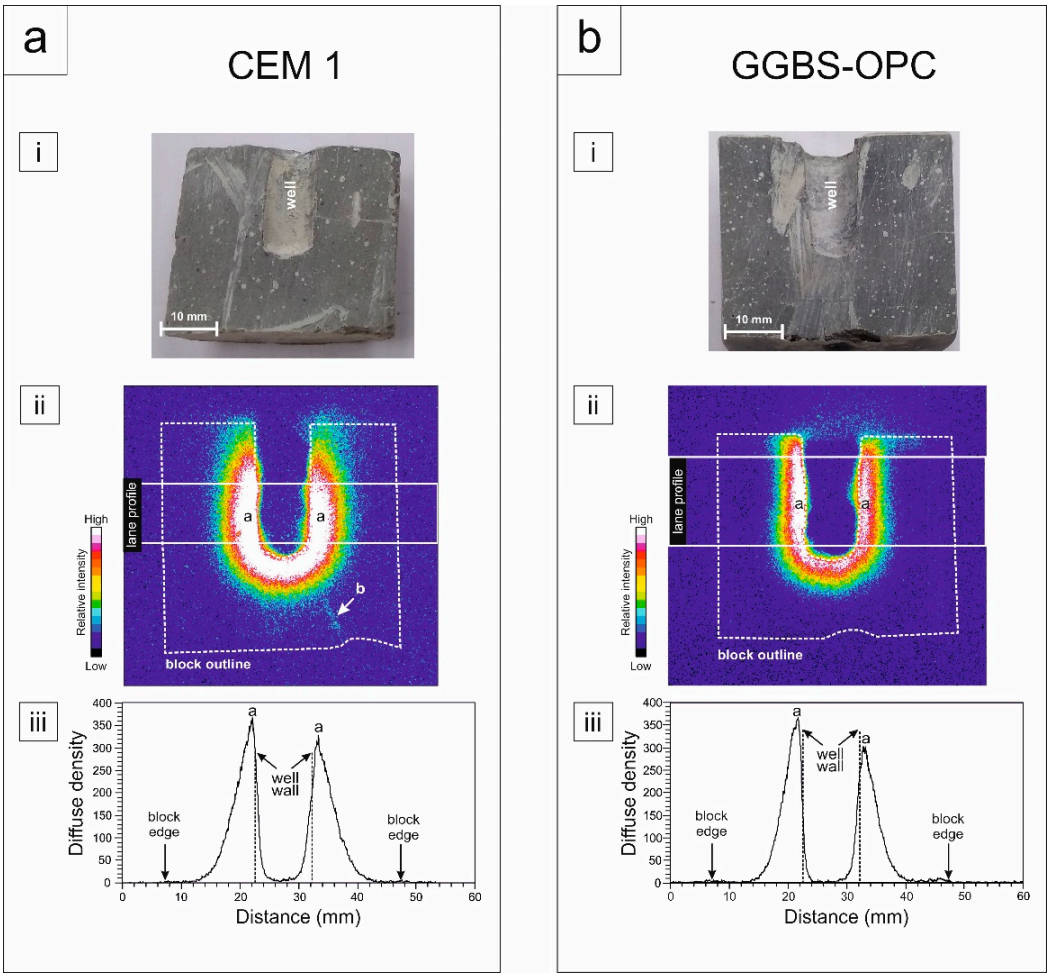

Figure 4. LPSL autoradiography results for ^{36}Cl distribution in (**a**) CEM I and (**b**) GGBS–OPC HCP blocks. Each diagram shows (i) a photograph of the longitudinally sawn surface of the HCP block; (ii) corresponding 16-colour contoured linearised LPSL autoradiograph; (iii) profile of the variation in radioactivity across the block (corrected for "average background"), measured along the "lane" drawn in (ii). The locations of peak distributions in radioactivity (labelled "a") are shown in each of the LPSL autoradiograph images and the corresponding lane profiles. The feature labelled "b" in the CEM I HCP block corresponds to radioactivity along a microfracture in the HCP block.

Autoradiography analyses of Cebama HCP block (Figure 5a) and the NRVB HCP block (Figure 5b) show broadly similar patterns for the ^{36}Cl activity distribution. The ^{36}Cl was observed to have diffused throughout both HCP blocks. However, the Cebama block revealed stronger retention of ^{36}Cl, with overall higher activity compared to the NRVB HCP, although this retention is significantly lower than in either the CEM I or GGBS–OPC HPC (cf. Figure 4). For the Cebama block, the ^{36}Cl activity reaches a peak at a depth of between 4 and 6 mm from the well wall (feature labelled "a" in Figure 5a) and progressively decreases over a broad interval towards background activity levels at the very edge of the block. The autoradiography also revealed a slight increase in radioactivity at the outer edge on one side of the block (Figure 5a(iii)), which may indicate that there has been some local back-reaction or resorption of ^{36}Cl from the surrounding fluid during the experiment. The NRVB cement displayed a broad peak in ^{36}Cl activity, approximately half the intensity of that in the Cebama HCP but at a shallower depth of 2–3 mm from the wall of the central well (feature labelled "a" in Figure 5b). The ^{36}Cl activity falls to a relatively low level at about 8 mm from the well wall (within the middle of the HCP block itself), within a much smaller interval than was observed in the Cebama block. A slight increase in ^{36}Cl activity (above background) is just discernible towards the edge of the NRVB block (Figure 5b(iii)), which might indicate some local back-reaction or resorption of ^{36}Cl from

the surrounding fluid during the experiment (as was also noted for the Cebama HCP). Again, these autoradiography results are consistent with the through-diffusion data, which showed significant out-diffusion of ^{36}Cl from both the Cebama and NRVB HCP, with the NRVB cement showing the greater diffusive flux of ^{36}Cl (cf. Figure 3).

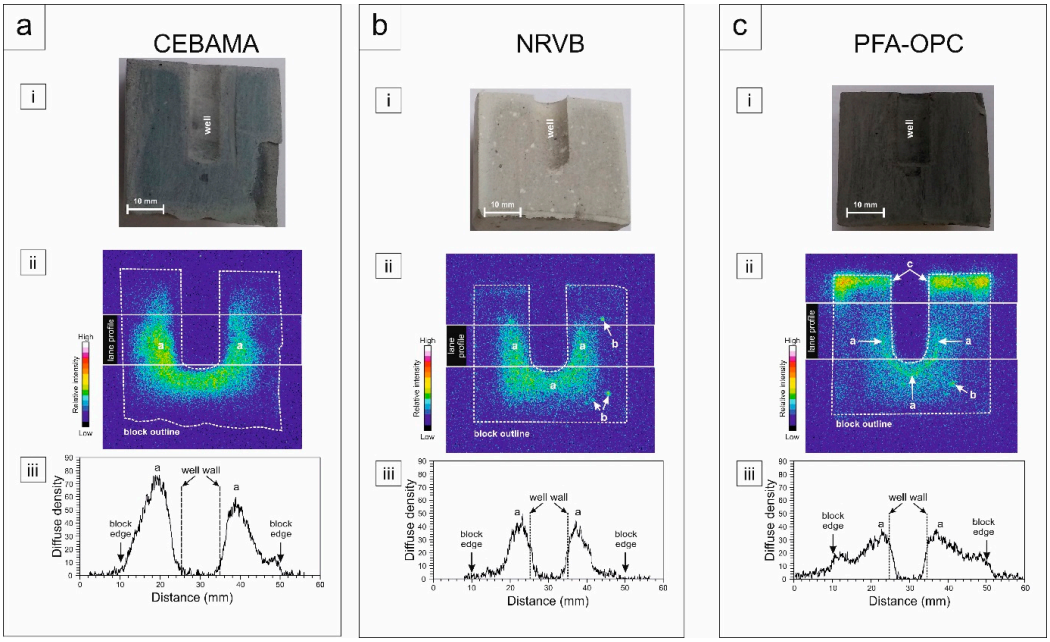

Figure 5. LPSL autoradiography results for ^{36}Cl distribution in (**a**) Cebama; (**b**) NRVB; and (**c**) PFA–OPC HCP blocks. Each diagram shows (i) a photograph of the longitudinally sawn surface of the cement block; (ii) corresponding 16-colour contoured linearised LPSL autoradiograph; (iii) profile of the variation in radioactivity across the block (corrected for "average background" radioactivity), measured along the "lane" drawn in (ii). The locations of peak distributions in radioactivity (labelled "a") are shown in each of the LPSL autoradiograph images and the corresponding lane profiles. Occasional discrete radioactive "hot-spots" (labelled "b") can be seen in the NRVB and PFA–OPC HPC blocks. A horizontal region of enhanced radioactivity (labelled "c") can be clearly seen towards the top of the PFA–OPC sample.

Autoradiography results from the PFA–OPC block show a very diffuse distribution of low-level activity from ^{36}Cl throughout this block (Figure 5c). The activity distribution shows a very broad peak within the HCP, at a depth of between 2 and 3 mm from the central well, which decreases progressively over a broad distance to the edge of the HCP block. The overall activity is lower than in the Cebama and NRVB HCP blocks, demonstrating poor retention of ^{36}Cl by the PFA–OPC HCP, consistent with the high ^{36}Cl flux observed in the diffusion experiment (cf. Figure 3). As also seen in both the Cebama and NVRB blocks, the ^{36}Cl activity increases slightly towards the edges of the HCP block (Figure 5c(iii)), indicating some back-reaction/resorption of ^{36}Cl from the fluid phase surrounding the block. The autoradiograph image of the PFA–OPC block also showed a marked enhancement of activity from ^{36}Cl, within a narrow horizon 2–7 mm thick at the very top of the block (feature labelled "c" in Figure 5c(ii)). This feature may be an artefact produced by capillary migration of porewater towards the upper surface of the cement block, as the block dried out after the end of the experiment. However, this also demonstrates that the ^{36}Cl is very mobile and is not bound or strongly retained within the matrix of this cementitious material.

The few discrete "hot-spots" identified in the autoradiographs from the NRVB and the PFA–OPC blocks (Figure 5b and 5c) may correspond to discrete cement clinker particles that the ^{36}Cl has interacted with within these two HCP. Effects of microcracks as po-

tential preferential radionuclide pathways were only rarely observed (Figure 4a); however, the microfractures in the cement block seemed not to reach the outer edges of the cylinders.

4. Discussion

^{36}Cl is considered as one of the most important dose-relevant radionuclides in many waste disposal scenarios. Therefore, its interaction with cement-based engineered barriers is of particular relevance (e.g., [23,47]). In the repository environment, the retention of ^{36}Cl is expected to occur mainly due to interaction with the cement hydration phases as the precipitation of Cl-bearing phases, such as Friedel's salt or calcium oxychlorides, occurs only at Cl^- concentrations exceeding the millimole level [11].

The results of the batch sorption experiments with single hydration phases revealed only a relatively weak uptake of Cl^- in line with the observations in Ochs et al. [11], which, in the case of the C-S-H, can probably be attributed to electrostatic sorption phenomena. At Ca/Si ratios below 1.2, the surface charge of C-S-H becomes negative, favouring uptake of cations [11]. For C-S-H0.9, a zeta potential of approx. −5 mV can be assumed based on data in [48]. The R_d value determined for C-S-H0.9 is in the same order of magnitude as those observed by Sugiyama and Fujita [49] for C-S-H with low Ca/Si-ratios (R_d between 2.8 and 19 L kg^{-1}). The R_d value of AFm-SO_4 is similar to the one found by Aggarwal et al. [30] for hydrotalcite (R_d = 32 L kg^{-1}) and might be due to the formation of Friedel's salt or the formation of Cl^--bearing AFm solid solutions (cf. [11,28]). Fujiwara et al. [50] determined a somewhat lower R_d for monosulphate (13 L kg^{-1}) in pure water. The lower Cl^- uptake by AFm-CO_3 compared to AFm-SO_4 indicates the influence of the interlayer anion and its geometry (SO_4: tetrahedral; CO_3: planar) as well its hydration (and the number of H_2O molecules in the interlayer, respectively) on the anion exchange by AFm phases. Similar effects of the interlayer anion on the anion uptake by AFm and structurally related hydrotalcite-like layered double hydroxides have been observed also in other systems, e.g., regarding the uptake of halogen and selenium species [17,23,51].

The R_d values determined for the different HCP (Table 3) are consistent with data reported in the literature for similar materials, considering also the well-known phenomenon of reduced sorption with increasing Cl^- concentration in the pore water, which has been discussed in detail elsewhere [11,52]. Ochs et al. [11] reported a range of R_d values for chloride for OPC-based cementitious systems in degradation state I (pH > 12.5) between 0.2 and 50 L kg^{-1}, with a suggested best estimate of 20 L kg^{-1} for total chloride concentrations of < 1 mM. In batch sorption experiments with HCP CEM I, Pointeau et al. [42] determined R_d values between 9.4 and 48 L kg^{-1} at pH > 12.5. Through-diffusion experiments with HCP prepared from sulphate-resistant Portland cement revealed R_d values between 26 and 49 L kg^{-1} [53,54]. Recently, Nedyalkova et al. [55] determined R_d values of 17 and 23 L kg^{-1} for sorption of ^{36}Cl on fresh OPC-based HCP in kinetic and isotherm experiments, respectively. Sorption experiments with NRVB [30,56] revealed distribution coefficients between 1 and 30 L kg^{-1}—the lower values determined at Cl^- concentrations of 0.5 M—in line with our results. In contrast, the R_d values for a 3:1 PFA–OPC blend and a 9:1 GGBS–OPC blend are distinctly higher than those determined by Aggarwal et al. [30] for similar blends (R_d = 1 L kg^{-1} and 2.5 L kg^{-1}, respectively).

The diffusive movement of radionuclides through a (nano)porous medium such as HCP is governed by a combination of physical (constrictivity, tortuosity, and pore architecture) and chemical processes ("sorption"). Tritiated water (HTO) was used in our experiments to attempt to distinguish between these two. HTO is often regarded as a conservative tracer; however, it can undergo isotopic exchange with the hydrogen bound in the solid hydration phases, such as C-S-H, which thus retards migration, allowing for a greater time to interact with the cementitious material. Despite the limitations of this approach, differences in tritium transport rates provide an indication of HCP diffusivity. As indicated by the HTO fluxes, the rate of diffusive transport in the HCP could be expected to decrease in the order PFA–OPC ≈ NRVB > Cebama >> CEM I ≈ GGBS–OPC. The higher

diffusivity of NRVB compared to most of the other HCP is probably due to the higher w/c ratio of 0.55, which leads to an increase in porosity and a higher percentage of capillary pores, thus facilitating solute transport. Surprisingly, the HCP made from CEM I showed similar transport properties to the 9:1 GGBS–OPC blend; usually, it is assumed that the pore structure of blast furnace slag cements is more refined than those of CEM I, leading to lower diffusivities. In this context, the higher HTO flux observed for the Cebama reference mix compared to the CEM I is notable, since the addition of GGBS and SF should also result in low effective diffusivities. However, this effect might be due to the young age of the HCP used in the diffusion experiment, since the hydration kinetics of this blend are known to be very slow, still containing unreacted clinker phases after 18 months of hydration [57]. Generally, it can be assumed that the CEM I HCP is more hydrated compared to the blended cements. Thus, the diffusivities of the HCPs made from blended cements might decrease with ongoing hydration so that the differences with the CEM I HCP in ^{36}Cl transport in "real" applications might be lower than indicated from our diffusion experiments.

The through-diffusion experiments with HTO and ^{36}Cl and the complementary autoradiography results provide a consistent picture on the migration behaviour of this radionuclide in cementitious systems. In the diffusion experiments with HCP prepared from CEM I and GGBS–OPC no ^{36}Cl flux into the outside reservoir was observed during the experiment; all the ^{36}Cl is retained inside the cylinder close to the well walls. This indicates strong retention of ^{36}Cl in these cement formulations and very limited ^{36}Cl migration in the experiments, correlating to the lower effective HTO diffusivities in these materials. The autoradiography analyses of the Cebama HCP and the NRVB HCP are broadly similar with respect to the ^{36}Cl activity distribution, with stronger ^{36}Cl retention in the Cebama HPC. However, in both cases, ^{36}Cl diffused throughout the HPC blocks during the experiments with higher fluxes (lower overall retention) of ^{36}Cl in the case of the NRVB, probably affected by the higher w/c used for this material and thus higher porosity and effective diffusivity. The PFA–OPC HCP showed the lowest transport resistance with respect to HTO and consequently also the highest ^{36}Cl fluxes, with a very weak ^{36}Cl retention in the cementitious matrix.

The observations from the through-diffusion experiments and the autoradiography, which can provide a more realistic picture of radionuclide migration behaviour in cementitious barriers, indicate a decreasing diffusive ^{36}Cl transport in the order PFA–OPC > NRVB > Cebama >> CEM I ≈ GGBS–OPC. Interestingly, this does not correlate with the measured R_d values, where PFA–OPC showed a distinctly higher R_d for Cl^- than the other HCPs. However, ^{36}Cl diffusion through and retention in the HCP monoliths show a consistent picture with HTO diffusion, which is governed by microstructural properties of the HCP (such as porosity, pore architecture, etc.). This suggests that other physical factors related to the microstructure of the HCP (porosity, pore size distribution, pore architecture, constrictivity, and tortuosity) and also potentially electrostatic surface effects (EDL effect) and anion exclusion can also play an important role with respect to the migration behaviour of weakly sorbing, anionic radionuclides in cementitious materials. This suggests that distribution ratios (R_d values) alone are unreliable indicators of the transport behaviour of these radionuclides in cementitious matrices.

Regarding the selection of binders for cementitious barriers or for the solidification of radioactive waste streams, the results of this study suggest that formulations based on CEM I or GGBS–OPC blends would be favourable with respect to the retention of ^{36}Cl, decreasing its migration length. Based on the similar behaviour of iodide in cementitious environments (e.g., [11,55]), these cementitious materials could also limit the migration of ^{129}I in the repository environment. With both binders discussed, GGBS–OPC might be also beneficial with respect to the retention of redox-sensitive anionic radionuclides such as Tc(VII), given its potential reduction in the presence of Fe(II) and sulphides in the slag.

5. Conclusions

Batch experiments on individual hydration phases present in cementitious materials based on OPC and blended cements point to a limited uptake of ^{36}Cl by C-S-H and AFm, due to electrostatic sorption processes and anion exchange in the interlayer, respectively. Sorption distribution ratios (R_d) for chloride determined on HCP samples, representative of cementitious materials considered for use in geological disposal facilities throughout Europe, were found to be in the range between 6 and 26 L kg^{-1}, with the highest Cl^- retention provided by a PFA–OPC blend. However, the diffusion of ^{36}Cl through cured monolithic HCP samples revealed markedly diverse migration behaviour of ^{36}Cl, not directly correlated to the R_d values. This suggests that physical factors related to the microstructure can also have a significant effect on the diffusion behaviour of weakly sorbing anionic radionuclides, making R_d values alone unreliable predictors for their migration behaviour. Two of the matrices, based on a GGBS–OPC blend and pure CEM I, respectively, effectively retarded ^{36}Cl migration, retaining the radionuclide in narrow, reactive zones. These findings have implications when selecting cementitious grouts and/or backfill materials for ^{36}Cl-bearing radioactive wastes.

Supplementary Materials: The following supporting information can be downloaded at: https://www.mdpi.com/article/10.3390/min14101017/s1, Table S1: Major element oxides in the constituents used to prepare the cement pastes; Table S2: Composition of aqueous solutions equilibrated with HCP used in batch sorption and through diffusion experiments [44]; Table S3: pH of aqueous solutions equilibrated with synthesised cement hydration phases [34]; Figure S1: (a) XRD pattern of C-S-H0.9 and (b) SEM image (back-scattered electron mode) of C-S-H0.9 [34]; Figure S2: (a) XRD pattern of AFm-SO_4 and (b) SEM image (back-scattered electron mode) of AFm-SO_4 [34]; Figure S3: (a) XRD pattern of AFm-CO_3 and (b) SEM image (back-scattered electron mode) of AFm-CO_3 [34].

Author Contributions: Conceptualisation, D.R., A.E.M., and G.D.; methodology, M.I., S.L., and A.E.M.; validation, D.R. and D.B.; formal analysis, M.I., S.L., and A.E.M.; investigation, M.I., S.L., and A.E.M.; resources, D.R. and D.B.; data curation, M.I., S.L., and A.E.M.; writing—original draft preparation, G.D., D.R., and A.E.M.; writing—review and editing, M.I., S.L., A.E.M., G.D., and D.B.; supervision, D.R. and D.B.; project administration, D.R. and G.D.; funding acquisition, D.B. and D.R. All authors have read and agreed to the published version of the manuscript.

Funding: The research leading to these results has received funding from the European Union's Horizon 2020 Research and Training Programme of the European Atomic Energy Community (EURATOM) (H2020-NFRP-2014/2015) under grant agreement n° 662147 (CEBAMA).

Data Availability Statement: Data are contained within the article or Supplementary Materials.

Acknowledgments: Tapio Vehmas and Markku Leivo from VTT Technical Research Centre of Finland are acknowledged for providing samples and constituents of the Cebama low-pH reference cement paste. AEM publishes with the permission of the Executive Director of the British Geological Survey (United Kingdom Research and Innovation, UKRI).

Conflicts of Interest: The authors declare that the research was conducted in the absence of any commercial or financial relationships that could be construed as a potential conflict of interest.

References

1. Glasser, F.P. Application of inorganic cements to the conditioning and immobilisation of radioactive wastes. In *Handbook of Advanced Radioactive Waste Conditioning Technologies*; Ojovan, M.I., Ed.; Woodhead: Oxford, UK, 2011; pp. 67–135.
2. Bel, J.P.; Wickham, S.M.; Gens, R.M.F. Development of the supercontainer design for deep geological disposal of high-level heat emitting radioactive waste in Belgium. *Mater. Res. Soc. Symp. Proc.* **2006**, *932*, 1221. https://doi.org/10.1557/PROC-932-122.1.
3. Drace, Z.; Ojovan, M.I. A Summary of IAEA coordinated research project on cementitious materials for radioactive waste management. In *Cement-Based Materials for Nuclear Waste Storage*; Bart, F., Cau-dit-Coumes, C., Frizon, F., Lorente, S., Eds.; Springer: New York, NY, USA, 2013; pp. 3–11.
4. Duro, L.; Altmaier, M.; Holt, E.; Mäder, U.; Claret, F.; Grambow, B.; Idiart, A.; Valls, A.; Montoya, V. Contribution of the results of the CEBAMA project to decrease uncertainties in the Safety Case and Performance Assessment of radioactive waste repositories. *Appl. Geochem.* **2020**, *112*, 104479. https://doi.org/10.1016/j.apgeochem.2019.104479.

5. Bach, T.; Pochard, I.M.; Cau-dit-Coumes, C.; Mercier, C.; Nonat, A. Prediction of long-term chemical evolution of a low-pH cement designed for underground radioactive waste repositories. In *Cement-Based Materials for Nuclear Waste Storage*; Bart, F., Cau-dit-Coumes, C., Frizon, F., Lorente, S., Eds.; Springer: New York, NY, USA, 2013; pp. 239–250.
6. Cau Dit Coumes, C.; Courtois, S.; Nectoux, D.; Leclercq, S.; Bourbon, X. Formulating a low-alkalinity, high-resistance and low-heat concrete for radioactive waste repositories. *Cem. Concr. Res.* **2006**, *36*, 2152–2163. https://doi.org/10.1016/j.cemconres.2006.10.005.
7. Codina, M.; Cau-dit-Coumes, C.; Le Bescop, P.; Verdier, J.; Ollivier, J.P. Design and characterization of low-heat and low-alkalinity cements. *Cem. Concr. Res.* **2008**, *38*, 437–448. https://doi.org/10.1016/j.cemconres.2007.12.002.
8. Lothenbach, B.; Le Saout, G.; Ben Haha, M.; Figi, R.; Wieland, E. Hydration of a low-alkali CEM III/B–SiO_2 cement (LAC). *Cem. Concr. Res.* **2012**, *42*, 410–423. https://doi.org/10.1016/j.cemconres.2011.11.008.
9. Glasser, F.P. Mineralogical aspects of cement in radioactive waste disposal. *Mineral. Mag.* **2001**, *65*, 621–633. https://doi.org/10.1180/002646101317018442.
10. Taylor, H.F.W. *Cement Chemistry*, 2nd ed.; Thomas Telford: London, UK, 1997; 459p.
11. Ochs, M.; Mallants, D.; Wang, L. *Radionuclide and Metal Sorption on Cement and Concrete*; Springer: Cham, Switzerland, 2016; 301p.
12. Glasser, F.P. Fundamental aspects of cement solidification and stabilization. *J. Hazard. Mater.* **1997**, *52*, 151–170. https://doi.org/10.1016/S0304-3894(96)01805-5.
13. Evans, N.D.M. Binding mechanisms of radionuclides to cement. *Cem. Concr. Res*. **2008**, *38*, 543–553. https://doi.org/10.1016/j.cemconres.2007.11.004.
14. Gougar, M.L.D.; Scheetz, B.E.; Roy, D.M. Ettringite and C-S-H Portland cement phases for waste ion immobilization: A review. *Waste Manag*. **1996**, *16*, 295–303. https://doi.org/10.1016/S0956-053X(96)00072-4.
15. Heath, T.G.; Illet, D.J.; Tweed, C.J. *Development of a Near-Field Sorption Model for a Cementitious Repository*; UK Nirex Report AEAT/R/ENV/0229; AEA Technology: Harwell, UK, 2000.
16. Wang, L.; Ochs, M.; Mallants, D.; Vielle-Petit, L.; Martens, E.; Jacques, D.; de Cannière, P.; Berry, J.A.; Leterme, B. A new radionuclide sorption data base for benchmark cement accounting for geochemical evolution of cement. In *Cement-Based Materials for Nuclear Waste Storage*; Bart, F., Cau-dit-Coumes, C., Frizon, F., Lorente, S., Eds.; Springer: New York, NY, USA, 2013; pp. 103–112.
17. Wieland, E. *Sorption Data Base for the Cementitious Near Field of L/ILW And ILW Repositories for Provisional Safety Analyses for Sgt-E2*; Nagra Technical Report NTB 14-08; Nagra: Wettingen, Switzerland, 2014.
18. Wieland, E.; Van Loon, L.R. *Cementitious Near-Field Sorption Data Base for Performance Assessment of an ILW Repository in Opalinus Clay*; Nagra Technical Report NTB 02-20; Nagra: Wettingen, Switzerland, 2002.
19. Posiva. *Safety Case for the Disposal of Spent Nuclear Fuel at Olkiluoto*; Posiva Report 2012-12; Posiva Oy: Eurajoki, Finland, 2012.
20. SKB. *Safety Analysis for SFR Long-Term Safety: Main Report for the Safety Assessment SR-PSU*; SKB Technical Report 14-01; Svensk Kärnbränslehantering AB: Stockholm, Sweden, 2015.
21. Brown, D.A.; Chadwick, M.B.; Capote, R.; Kahler, A.C.; Trkov, A.; Herman, M.W.; Sonzogni, A.A.; Danon, Y.; Carlson, A.D.; Dunn, M.; et al. ENDF/B-VIII.0: The 8th major release of the Nuclear Reaction Data Library with CIELO-project cross sections, new standards and thermal scattering data. *Nucl. Data Sheets* **2018**, *148*, 1–142. https://doi.org/10.1016/j.nds.2018.02.001.
22. Hummel, W. *Chemistry of Selected Dose-Relevant Radionuclides*; Nagra Technical Report NTB 17-05; Nagra: Wettingen, Switzerland, 2017.
23. Grambow, B.; López-García, M.; Olmeda, J.; Grivé, M.; Marty, N.C.M.; Grangeon, S.; Claret, F.; Lange, S.; Deissmann, G.; Klinkenberg, M.; et al. Retention of radionuclides on cementitious systems: Main outcome of the CEBAMA project. *Appl. Geochem*. **2020**, *112*, 104480. https://doi.org/10.1016/j.apgeochem.2019.104480.
24. Beaudoin, J.J.; Ramachandran, V.S.; Feldman, R.F. Interaction of chloride and C-S-H. *Cem. Concr. Res*. **1990**, *20*, 875–883. https://doi.org/10.1016/0008-8846(90)90049-4.
25. Viallis, H.; Faucon, P.; Petit, J.C.; Nonat, A. Interaction between salts (NaCl, CsCl) and calcium silicate hydrates (C-S-H). *J. Phys. Chem. B* **1999**, *103*, 5212–5219.
26. Sugiyama, D. Chemical alteration of calcium silicate hydrate (C-S-H) in sodium chloride solution. *Cem. Concr. Res*. **2008**, *38*, 1270–1275. https://doi.org/10.1016/j.cemconres.2008.06.002.
27. Birnin-Yauri, U.; Glasser, F. Friedel's Salt, $Ca_2Al(OH)_6(Cl,OH)\cdot 2H_2O$: Its solid solutions and their role in chloride binding. *Cem. Concr. Res.* **1998**, *28*, 1713–1723. https://doi.org/10.1016/S0008-8846(98)00162-8.
28. Balonis, M.; Lothenbach, B.; Le Saout, G.; Glasser, F.P. Impact of chloride on the mineralogy of hydrated Portland cement systems. *Cem. Concr. Res.* **2010**, *40*, 1009–1022. https://doi.org/10.1016/j.cemconres.2010.03.002.
29. Van Es, E.; Hinchliff, J.; Felipe-Sotelo, M.; Milodowski, A.E.; Field, L.P.; Evans, N.D.M.; Read, D. Retention of chlorine-36 by a cementitious backfill. *Mineral. Mag.* **2015**, *79*, 1297–1305. https://doi.org/10.1180/minmag.2015.079.6.05.
30. Aggarwal, S.; Angus, M.J.; Ketchen, J. *Sorption of Radionuclides onto Specific Mineral Phases Present in Repository Cements*; AEA Technology Report NSS/R312, AEA-D&R-0395; AEA Technology PLC, Windscale: Cumbria, UK, 2000.
31. Atkins, M.; Glasser, F.P.; Kindness, A. Cement hydrate phases: Solubility at 25 °C. *Cem. Concr. Res.* **1992**, *22*, 241–246. https://doi.org/10.1016/0008-8846(92)90062-Z.
32. Baur, I.; Keller, P.; Mavrocordatos, D.; Wehrli, B.; Johnson, C.A. Dissolution-precipitation behaviour of ettringite, monosulfate, and calcium silicate hydrate. *Cem. Concr. Res.* **2004**, *34*, 341–348. https://doi.org/10.1016/j.cemconres.2003.08.016.

33. Matschei, T.; Lothenbach, B.; Glasser, F.P. The AFm phase in Portland cement. *Cem. Concr. Res.* **2006**, *37*, 118–130. https://doi.org/10.1016/j.cemconres.2006.10.010.
34. Lange, S. Structural Uptake and Retention of Safety Relevant Radionuclides by Cementitious Materials. Ph.D. Thesis, RWTH Aachen University, Aachen, Germany, 2019.
35. Lange, S.; Kowalski, P.; Pšeničkа, M.; Klinkenberg, M.; Rohmen, S.; Bosbach, D.; Deissmann, G. Uptake of ^{226}Ra in cementitious systems: A complementary solution chemistry and atomistic simulation study. *Appl. Geochem.* **2018**, *96*, 204–216. https://doi.org/10.1016/j.apgeochem.2018.06.015.
36. Lange, S.; Klinkenberg, M.; Barthel, J.; Bosbach, D.; Deissmann, G. Uptake and retention of molybdenum in cementitious systems. *Appl. Geochem.* **2020**, *119*, 104630. https://doi.org/10.1016/j.apgeochem.2020.104630.
37. Francis, A.J.; Cather, R.; Crossland, I.G. 1997. Nirex Safety Assessment Research Programme: Development of the Nirex Reference Vault Backfill; Report on Current Status in 1994. UK NIREX Report no: S/97/014, United Kingdom Nirex Ltd., Harwell, Oxfordshire, UK.
38. Vehmas, T.; Schnidler, A.; Löija, M.; Leivo, M.; Holt, E. Reference mix design and castings for low-pH concrete for nuclear waste repositories. *KIT Sci. Rep.* **2017**, *7734*, 101–111.
39. Vehmas; T.; Montoya, V.; Alonso, M.C.; Vasícek, R.; Rastrick, E.; Gaboreau, S.; Vecerník, P.; Leivo, M.; Holt, E.; Fink, N.; Ait Mouheb, N.; et al. Characterization of Cebama low-pH reference concrete and assessment of its alteration with representative waters in radioactive waste repositories. *Appl. Geochem.* **2020**, *121*, 104703. https://doi.org/10.1016/j.apgeochem.2020.104703.
40. Leivo, M.; Vehmas, T.; Holt, E. Developing low pH concrete for tunnel plugging structures in nuclear waste containment. In Proceedings of the XIII Nordic Concrete Research Symposium, Reykjavik, Iceland, 13–15 August 2014.
41. Holt, E.; Koho, P. POPLU Experimental Summary Report. Deliverable D4.5, DOPAS Project (Contract Number: FP7–323273), 2016. Available online: https://www.posiva.fi/dopas/en/dopas/deliverables.html (accessed on 20 August 2024).
42. Pointeau, I.; Coreau, N.; Reiller, P.E. Uptake of anionic radionuclides onto degraded cement pastes and competing effect of organic ligands. *Radiochim. Acta* **2008**, *96*, 367–374. https://doi.org/10.1524/ract.2008.1503.
43. Felipe-Sotelo, M.; Hinchliff, J.; Drury, D.; Evans, N.D.M.; Williams, S.; Read, D. Radial diffusion of radiocaesium and radioiodide through cementitious backfill. *Phys. Chem. Earth* **2014**, *70–71*, 60–70. https://doi.org/10.1016/j.pce.2014.04.001.
44. Isaacs, M.; Lange, S.; Deissmann, G.; Bosbach, D.; Milodowski, A.E.; Read, D. Retention of technetium-99 by grout and backfill cements: Implications for the safe disposal of radioactive waste. *Appl. Geochem.* **2020**, *116*, 104580. https://doi.org/10.1016/j.apgeochem.2020.104580.
45. Rasband, W.S. *ImageJ*, Version 1.48k; US National Institutes of Health: Bethesda, MD, USA, 2013. Available online: https://imagej.net (accessed on 04 July 2016).
46. Cathelin, R. *Linearize GelData*. SIGENAE Team, INRA: Toulouse, France, 2013. Available online: https://imagej.net/ij/plugins/linearize-gel-data.html (accessed on 20 January 2017).
47. Nagra. *Project Opalinus Clay—Safety Report. Demonstration of Disposal Feasibility for Spent Fuel, Vitrified High-Level Waste and Long-Lived Intermediate Level Waste*; Nagra Technical Report NTB 02-05; Nagra: Wettingen, Switzerland, 2002.
48. Viallis-Terris, H.; Nonat, A.; Petit, J.C. Zeta-potential study of calcium silicate hydrates interacting with alkaline cations. *J. Colloid Interface Sci.* **2001**, *244*, 58–65. https://doi.org/10.1006/jcis.2001.7897.
49. Sugiyama, D.; Fujita, T. *Chemical Alteration of Calcium Silicate Hydrates in Saline Groundwater—Mechanism of Sorption of Na on C-S-H and effect of NaCl on Leaching of Ca from C-S-H*; CRIEPI Report T03056; Central Research Institute of Electric Power Industry: Tokyo, Japan, 2004.
50. Fujiwara, K.; Saito, N.; Kaneko, M.; Toyohara, N.; Mitsuka, T.; Toyota, F.; Ikenaga, N. Fixation technique of radioiodine by cement. *J. Nucl. Fuel Cycle Environ.* **1999**, *6*, 75–78.
51. Rojo, H.; Scheinost, A.C.; Lothenbach, B.; Laube, A.; Wieland, E.; Tits, J. Retention of selenium by calcium aluminate hydrate (AFm) phases under strongly-reducing radioactive waste repository conditions. *Dalton Trans.* **2018**, *47*, 4209–4218. https://doi.org/10.1039/c7dt04824f.
52. Nielsen, E.P.; Herfort, D.; Geiker, M.R. Binding of chloride and alkalis in Portland cement systems. *Cem. Concr. Res*. **2005**, *35*, 117–123. https://doi.org/10.1016/j.cemconres.2004.05.026.
53. Sarott, F.A.; Bradbury, M.H.; Pandolfo, P.; Spieler, P. Diffusion and adsorption studies on hardened cement paste and the effect of carbonation on diffusion rates. *Cem. Concr. Res.* **1992**, *22*, 439–444. https://doi.org/10.1016/0008-8846(92)90086-B.
54. Jakob, A.; Sarott, F.A.; Spieler, P. *Diffusion and Sorption on Hardened Cement Pastes—Experiments and Modelling Results*; PSI-Bericht Nr. 99-05; Paul-Scherrer-Institut: Villingen, Switzerland, 1999.
55. Nedyalkova, L.; Tits, J.; Bernard, E.; Wieland, E.; Mäder, U. Sorption experiments with HTO, 36-Cl, 125-I and 14-C labeled formate on aged cement matrices retrieved from long-term in-situ rock laboratory experiments. *J. Adv. Concr. Technol.* **2021**, *19*, 811–829. https://doi.org/10.3151/jact.19.811.

56. Baker, S.; McCrohon, R.; Oliver, P.; Pilkington, N.J. The sorption of niobium, tin, iodine and chlorine onto NIREX reference vault backfill. *Mater. Res. Soc. Symp. Proc.* **1994**, *333*, 719–724. https://doi.org/10.1557/PROC-333-719.
57. Vasconcelos, R.; Walkley, B.; Day, S.; Tang, C.C.; Paraskevoulakos, H.; Gardner, L.J.; Corkhill, C.L. 18-month hydration of a low-pH cement for geological disposal of radioactive waste: The Cebama reference cement. *Appl. Geochem.* **2020**, *116*, 104536. https://doi.org/10.1016/j.apgeochem.2020.104536.